ISBN: 978-3-95450-208-0 doi:10.18429/JACoW-IPAC2019-MOPGW074

NEW SPIRAL BEAM SCREEN DESIGN FOR THE FCC-hh INJECTION KICKER MAGNET *

A. Chmielińska†, CERN, Geneva, Switzerland, EPFL, Lausanne, Switzerland
M. J. Barnes, CERN, Geneva, Switzerland

Abstract

The injection kicker system for the Future Circular Collider (FCC-hh) must satisfy demanding requirements. To achieve low pulse ripple and fast field rise and fall times, the injection system will use ferrite loaded transmission line type magnets. The beam coupling impedance of the kicker magnets is crucial, as this can be a dominant contribution to beam instabilities. In addition, interaction of the high intensity beam with the real part of the longitudinal beam coupling impedance can result in high power deposition in the ferrite yoke. This gives a significant risk that the ferrite yoke will exceed its Curie temperature: hence, a suitable beam screen will be a critical feature. In this paper, we present a novel concept - a spiral beam screen. The fundamental advantage of the new design is a significant reduction of the maximum voltage induced on the screen conductors, thus decreased probability of electrical breakdown. In addition, the longitudinal beam coupling impedance is optimized to minimize power deposition in the magnet.

INTRODUCTION

The FCC-hh will have two injection kicker systems to inject counter rotating proton beams. Each system will consist of 18 transmission line kicker magnets [1]. Each kicker magnet will have 20 cells. A cell consists of a C-core NiZn ferrite sandwiched between two high voltage (HV) capacitance plates: a plate connected to ground is situated between the two HV plates. The baseline material considered for the magnet yoke is CMD5005 ferrite [2], isostatically pressed, with a Curie temperature $T_C \geq 125$°C [3].

To limit power deposition in the ferrite yoke, a beam screen will be placed in the aperture of each kicker magnet [1]. The beam screen has to satisfy conflicting requirements of low beam coupling impedance, good high voltage performance, fast field rise and fall times with low ripple, low secondary electron yield (SEY), good radiation resistance and the ability to withstand temperatures up to 350°C during bake-outs required for compatibility with the ultra-high vacuum.

The first option considered for the FCC-hh kicker magnet was a "conventional" beam screen (see Fig. 1), with straight conductors, used for the injection kicker magnets of the Large Hadron Collider (LHC MKI) [4]. However, due to HV and heating concerns, we have developed a new concept of the spiral beam screen. The new design has low beam coupling impedance and improved HV performance. Hence it is the baseline proposed for the FCC-hh.

* Work supported by the FCC project.
† agnieszka.chmielinska@cern.ch

CONVENTIONAL BEAM SCREEN

The conventional beam screen consists of 24 straight, NiCr, screen conductors (2.7 mm × 0.8 mm). They are inserted into grooved slots in the inner wall of a ceramic tube (99.7% alumina), which is placed in the magnet aperture. The screen conductors provide a path for the beam image current and screen the ferrite yoke from the electromagnetic field of the circulating beam. To preserve a fast magnetic field rise time, the conductors are capacitively coupled to a grounded metallic cylinder at the upstream end, at which the beam enters the kicker magnet, and are directly connected to ground at the downstream end (see Fig. 1). Ferrite rings are mounted around each end of the alumina tube. At the upstream end, they absorb the beam induced power before it is deposited in the ferrite yoke [5]. For FCC-hh, CMD10 ferrite [2] isostatically pressed ($T_C \geq 250$°C [3]) is a baseline material for the rings.

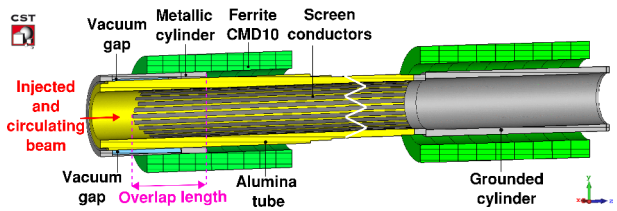

Figure 1: Schematic of the conventional beam screen.

Due to the capacitive coupling, an open-ended resonating cavity is formed in the region where the screen conductors overlap with the outer metallic cylinder. The n-th harmonic of the fundamental resonance occurs at the frequency [6]:

$$f_{\text{conv}}^{(n)} = \frac{nc}{2\sqrt{\varepsilon_{r,\text{eff}}}(L_{\text{overlap}} + \delta_{\text{fringe}})}, \quad (1)$$

where c is the speed of light, $\varepsilon_{r,\text{eff}}$ is the effective relative permittivity of the volume between the metallic cylinder and the overlap of the screen conductors, L_{overlap} is the length of the overlap between the metallic cylinder and longest screen conductor, and δ_{fringe} is the effective increase in length due to fringe fields. In the initial beam screen design for the FCC-hh injection kicker, $L_{\text{overlap}} = 56$ mm.

A significant voltage is induced on the screen conductors during the magnetic field rise and fall. The induced voltage on the i-th conductor is (see Fig. 2):

$$V_i = \frac{dB}{dt}(d + R - y_i)L, \quad (2)$$

where L is the length of a screen conductor within the uniform magnetic field B, R is the beam screen radius, d is the distance from the ground busbar (GND) and y_i is the coordinate of the screen conductor on the y-axis. HV breakdowns

Content from this work may be used under the terms of the CC BY 3.0 licence (© 2019). Any distribution of this work must maintain attribution to the author(s), title of the work, publisher, and DOI

This is a preprint — the final version is published with IOP

ISBN: 978-3-95450-208-0 doi:10.18429/JACoW-IPAC2019-MOPGW074

between adjacent screen conductors or between screen conductors and the metallic cylinder are a concern during the kicker operation [7]. Hence, to reduce the electric field at the upstream end, graded lengths of the screen conductors and a non-symmetric vacuum gap (1 mm to 3 mm) has been introduced as part of the "post-LS1" MKI design [8].

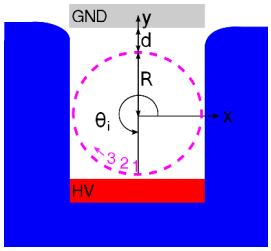

Figure 2: Cross-section of the beam screen.

NEW CONCEPT

The new concept of the spiral beam screen reduces beam coupling impedance and improves high voltage performance. In this design, the screen conductors are not straight, but each of them is twisted along the alumina tube. A schematic diagram of a single screen conductor is presented in Fig. 3.

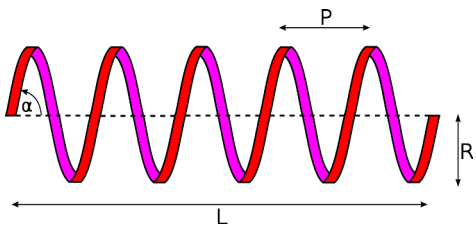

Figure 3: Schematic of a single spiral conductor.

Let us denote N_{turn} as the number of turns of the spiral conductor inside the length of the aperture of the kicker magnet. The length of the spiral inside the magnet aperture is:

$$s = \sqrt{L^2 + (2\pi R N_{\text{turn}})^2}. \tag{3}$$

As each screen conductor extends from the downstream to the upstream end of the beam screen, over a distance L_{total}, the total number of turns is given by: $N_{\text{total}} = \frac{L_{\text{total}}}{L} N_{\text{turn}}$. The pitch of the spiral is the distance which 1 turn of the spiral spans: $P = \frac{L}{N_{\text{turn}}}$. The angle of the spiral screen conductor is: $\alpha = \arctan(\frac{P}{2\pi R})$.

For the spiral beam screen, the coordinates of a point of the i-th screen conductor is described by:

$$\begin{cases} x_i(\theta) = R\cos(\theta + \theta_i) \\ y_i(\theta) = R\sin(\theta + \theta_i) \\ z_i(\theta) = \frac{P\theta}{2\pi};\ \theta \in [0; 2\pi N_{\text{turn}}], \end{cases} \tag{4}$$

where θ_i is the initial angle of the i-th screen conductor at the start of the cross-section (see Fig. 2). Assuming 24 conductors, $\theta_i = \frac{3}{2}\pi - \frac{2\pi(i-1)}{24}$. The distance from the GND busbar for the i-th screen conductor changes along the longitudinal direction and can be expressed as:

$$f_i(\theta) = d + R - y_i(\theta). \tag{5}$$

Note, $f_i(\theta)$ does not depend on x_i. To compute the induced voltage, for $\zeta = 2\pi N_{\text{turn}}$, let $k = \frac{dB}{dt}\frac{P}{2\pi}$, hence:

$$\begin{aligned} V_i &= k\int_0^{\zeta} f_i(\theta)d\theta = k\int_0^{\zeta}\Big(d + R - R\sin(\theta + \theta_i)\Big)d\theta \\ &= \frac{dB}{dt}(d+R)L - kR\Big(\cos(\theta_i) - \cos(\theta_i + \zeta)\Big). \end{aligned} \tag{6}$$

V_i is independent of θ_i when N_{turn} is an integer. In this case, the total induced voltage on each screen conductor is the same: $V_i = \frac{dB}{dt}(d+R)L$. This is approximately one-half of the worst case straight screen conductor: $V_1 = \frac{dB}{dt}(d+2R)L$. Also, for straight conductors, there can be a significant difference in the induced voltage between adjacent conductors, especially for $\theta \sim 0$ and $\sim \pi$. Whereas, for the spiral beam screen, there is no difference. Hence, a spiral beam screen is expected to provide significantly improved high voltage performance.

LONGITUDINAL IMPEDANCE OF THE SPIRAL BEAM SCREEN

From an analysis of the conventional design, the main resonances (see Eq. 1) are in good agreement for simulations performed for the kicker magnet with the beam screen (full model), just the beam screen (simplified model) and only the upstream end of the beam screen (cut-down model). The full model requires 2 weeks of computation on a high performance cluster, whereas the cut-down model is analyzed in 48 hours. For the spiral models, due to the lack of left-right symmetry present in the conventional design, the computation times double. Hence, the spiral beam screen was analyzed with a simplified or cut-down model (see Fig. 4).

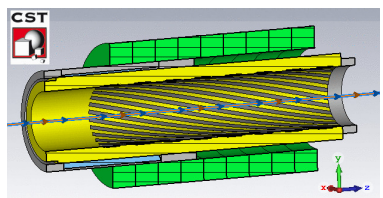

Figure 4: Spiral beam screen (cut-down model).

Benchmark predictions comparing the conventional design with the spiral design for different numbers of turns are shown in Fig. 5. Here, we consider a non-symmetric vacuum gap, ungraded screen conductors and $L_{\text{overlap}} = 56$ mm. The parameters of the spiral conductors are shown in Table 1. The length of a single screen conductor in the overlap region is denoted by x_{overlap}. The n-th harmonic of the fundamental resonance $f^{(n)}_{\text{spiral}}$ is determined by the overlap x_{overlap}. This becomes evident when comparing $f^{(n)}_{\text{conv}}/f^{(n)}_{\text{spiral}}$ with respect to $x_{\text{overlap}}/L_{\text{overlap}}$: the two ratios are in good agreement. Hence, Eq. 1 should be generalized by using x_{overlap} instead of L_{overlap} when the screen conductors are not straight. As x_{overlap} increases with the number of turns, the main harmonics shift to lower frequencies, which increases the power deposition. To address this, we propose to use the

This is a preprint — the final version is published with IOP
Content from this work may be used under the terms of the CC BY 3.0 licence (© 2019). Any distribution of this work must maintain attribution to the author(s), title of the work, publisher, and DOI

ISBN: 978-3-95450-208-0 doi:10.18429/JACoW-IPAC2019-MOPGW074

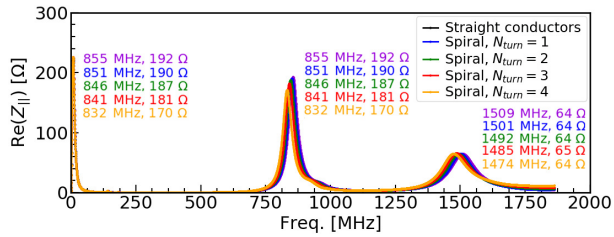

Figure 5: Real part of the longitudinal impedance of the spiral and conventional beam screen design (cut-down models).

spiral beam screen, with an integer number of turns over the effective length of the magnet, with conductors becoming straight in the overlap region.

Table 1: Parameters of the Spiral Beam Screen.

Parameter	Spiral			
N_{turn}	1	2	3	4
N_{total}	1.18	2.35	3.53	4.70
x_{overlap} [mm]	56.09	56.36	56.81	57.43
$x_{\text{overlap}}/L_{\text{overlap}}$	1.002	1.006	1.014	1.025
$f^{(1)}_{\text{conv}}/f^{(1)}_{\text{spiral}}$	1.004	1.011	1.015	1.027
$f^{(2)}_{\text{conv}}/f^{(2)}_{\text{spiral}}$	1.005	1.011	1.015	1.023

OPTIMIZATION

To improve the performance of the spiral beam screen in terms of heating, we reduced the overlap length from 56 mm to 44 mm, by shortening the screen conductors at the upstream end. Also, the vacuum gap is symmetrical, as this eliminates the quadrupolar component of transverse beam coupling impedance. Due to the spiral design, the total induced voltage, on each conductor, is equal to that of a conductor at a distance of $d + R$ from the GND busbar in the conventional beam screen. Hence, for HV reasons, the vacuum gap is equal to that at the vertical centre of the conventional design, i.e. 2 mm. In addition, as per the conventional design, the vacuum gap extends beyond all the screen conductors, to reduce the electric field [8].

Moreover, as the total induced voltage on each spiral conductor is nominally identical, and hence eddy currents should not circulate between conductors, we investigated a design with all spirals connected together in the overlap region. This idea is very interesting for future machines, e.g. the FCC-hh: if there was a "switch" to connect all screen conductors to the beam pipe, once injection is complete, there would be a continuous path for the beam image current and hence low beam coupling impedance. Whereas, for unconnected screen conductors, many "switches" would be necessary, which would increase cost and complexity.

Predictions for 44 mm overlap are shown in Fig. 6. The reduced overlap shifts the main harmonics to higher frequencies. The spiral design with conductors all connected together in the overlap region shifts the main harmonic to an even higher frequency. This is due to the length of the overlap being reduced from x_{overlap} to L_{overlap}.

For nominal FCC-hh beam parameters [9], the total power loss for the spiral models is between 31 W (for 1 turn) and 36 W (for 3 turns), while for the FCC-hh conventional design we expect 32 W. For spirals, a considerable contribution to the total power loss is between 100 MHz and 800 MHz (see the zoom in Fig. 6), where no resonances are expected to occur: hence these low-Q resonances are probably an artifact of the simulations with 3 turns but will be studied further. In all cases, the total power loss is lower than for the upgraded MKI with nominal LHC parameters (37 W, not scaled) [5]. In addition, similar power deposition distribution will occur in the FCC injection kicker magnets and the MKI's. Hence, since the upgraded MKI has not limited LHC operation [10], we conclude that heating of the FCC-hh injection kickers is acceptable too. However, the next step is to experimentally verify longitudinal beam impedance predictions. A prototype alumina tube with spiral screen conductors (see Fig. 7), applied using a copper paint, will be installed in a spare LHC MKI for beam coupling impedance measurements.

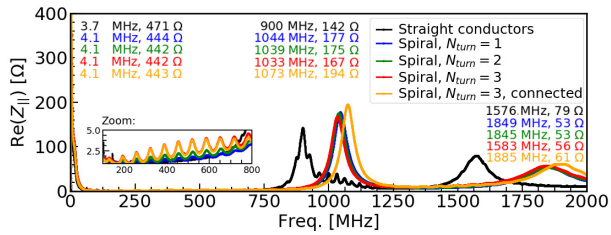

Figure 6: Real part of the longitudinal impedance for the spiral and conventional beam screens (simplified models).

Figure 7: Prototype of the spiral beam screen (photograph).

CONCLUSIONS

A novel, spiral, beam screen design has been presented which is expected to significantly improve the HV performance of the screen. Moreover, as the total voltage induced on each conductor is identical, the spiral conductors can be connected together in the overlap region - offering the possibility of a future substantial reduction in beam impedance. Improvements provided by the spiral beam screen, including simplicity of manufacture of the alumina tube, since grooves are no longer required, ensure that it will also be considered for kickers in accelerators other than FCC-hh.

ACKNOWLEDGEMENTS

The authors acknowledge F. Caspers for fruitful discussions. In addition, we would like to thank W. Weterings and G. Bellotto for help with preparation of the prototype. Special thanks to M. Alandes Pradillo and P. Llopis Sanmillan for good support with the computing infrastructure.

Content from this work may be used under the terms of the CC BY 3.0 licence (© 2019). Any distribution of this work must maintain attribution to the author(s), title of the work, publisher, and DOI

This is a preprint — the final version is published with IOP

ISBN: 978-3-95450-208-0 doi:10.18429/JACoW-IPAC2019-MOPGW074

REFERENCES

[1] A. Chmielińska *et al.*, "Preliminary estimate of beam induced power deposition in a FCC-hh injection kicker magnet", in *Proc. IPAC'17*, Copenhagen, Denmark, May 2017, paper WEPVA095, pp. 3475-3477.

[2] A. Chmielińska *et al.*, "Measurements of electromagnetic properties of ferrites as a function of frequency and temperature", in *Proc. IPAC'18*, Vancouver, Canada, May 2018, paper WEPMF089, pp. 2592-2595.

[3] National Magnetics Group, http://www.magneticsgroup.com

[4] H. Day, "Beam Coupling Impedance Reduction Techniques of CERN Kickers and Collimators", Ph.D. thesis, School of Physics and Astronomy, The University of Manchester, Manchester, United Kingdom, June 2013, CERN-THESIS-2013-083 (available online), p. 203.

[5] V. Vlachodimitropoulos, M.J. Barnes, A. Chmielińska, "Preliminary results from validation measurements of the longitudinal power deposition model for the LHC injection kicker magnet", in *Proc. IPAC'18*, Vancouver, Canada, May 2018, paper WEPMK005, pp. 2636-2639.

[6] H. Day *et al.*, "Beam coupling impedance of the new beam screen of the LHC injection kicker magnets", in *Proc. IPAC'14*, Dresden, Germany, June 2014, paper TUPRI030, pp. 1627-1629.

[7] M. J. Barnes *et al.*, "An improved beam screen for the LHC injection kickers", in *Proc. of PAC'07*, Albuquerque, USA, June 2007, TUPAN086, pp. 1574-1576

[8] M. J. Barnes *et al.*, "Reduction of surface flashover of the beam screen of the LHC injection kickers", in *Proc. of IPAC'13*, Shangai, China, May 2013, paper MOPWA032, pp. 735- 737.

[9] M. Benedikt *et al.*, "Future Circular Collider Study: The Hadron Collider (FCC-hh)", CERN, Geneva, Switzerland, Rep. ACC-2018-0058, December 2018, p. 14.

[10] M. J. Barnes *et al.*, "Operational Experience of a prototype LHC injection kicker magnet with a low SEY coating and redistributed power deposition", presented at IPAC19, Melbourne, Australia, May 2019, paper THPRB072, this conference.

This is a preprint — the final version is published with IOP

Content from this work may be used under the terms of the CC BY 3.0 licence (© 2019). Any distribution of this work must maintain attribution to the author(s), title of the work, publisher, and DOI